

Fossil evidence for serpentinization fluids fueling chemosynthetic assemblages

Franck Lartaud^{a,b,*}, Crispin T. S. Little^c, Marc de Rafelis^b, Germain Bayon^d, Jerome Dymont^e, Benoit Ildefonse^f, Vincent Gressier^b, Yves Fouquet^d, Françoise Gaill^g, and Nadine Le Bris^{a,h}

^a Université Pierre et Marie Curie–Paris 6, Laboratoire d'Ecogéochimie des Environnements Benthiques, Centre National de la Recherche Scientifique, Laboratoire Arago, 66650 Banyuls-sur-Mer, France

^b Université Pierre et Marie Curie–Paris 6, Institut des Sciences de la Terre de Paris, Laboratoire Biominéralisations et Environnements Sédimentaires, Centre National de la Recherche Scientifique 75252 Paris Cedex 05, France

^c School of Earth and Environment, University of Leeds, Leeds LS2 9JT, United Kingdom

^d Département Géosciences Marines, Institut Français de Recherche pour l'Exploitation de la Mer, Centre de Brest, 29280 Plouzané, France

^e Institut de Physique du Globe de Paris, Centre National de la Recherche Scientifique, Equipe Géosciences Marines, 75252 Paris Cedex 05, France

^f Géosciences Montpellier, Centre National de la Recherche Scientifique, Université Montpellier 2, 34095 Montpellier Cedex 05, France

^g Centre National de la Recherche Scientifique, Institut Écologie et Environnement, Université Pierre et Marie Curie, Institut de Recherche pour le Développement, Muséum National d'Histoire Naturelle, 75252 Paris Cedex 05, France

^h Laboratoire Environnements Profonds, Institut Français de Recherche pour l'Exploitation de la Mer, Centre de Brest, 29280 Plouzané, France

*: Corresponding author : Franck Lartaud, Tel : +334 30 19 24 14 ; Fax : +334 68 88 73 95 ;
email address : franck.lartaud@obs-banyuls.fr

Abstract :

Among the deep-sea hydrothermal vent sites discovered in the past 30 years, Lost City on the Mid-Atlantic Ridge (MAR) is remarkable both for its alkaline fluids derived from mantle rock serpentinization and the spectacular seafloor carbonate chimneys precipitated from these fluids. Despite high concentrations of reduced chemicals in the fluids, this unique example of a serpentinite-hosted hydrothermal system currently lacks chemosynthetic assemblages dominated by large animals typical of high-temperature vent sites. Here we report abundant specimens of chemosymbiotic mussels, associated with gastropods and chemosymbiotic clams, in approximately 100 kyr old Lost City-like carbonates from the MAR close to the Rainbow site (36°N). Our finding shows that serpentinization-related fluids, unaffected by high-temperature hydrothermal circulation, can occur on-axis and are able to sustain high-biomass communities. The widespread occurrence of seafloor ultramafic rocks linked to likely long-range dispersion of vent species therefore offers considerably more ecospace for chemosynthetic fauna in the oceans than previously supposed.

Keywords : *Bathymodiolus* ; Ghost City ; ultramafic-hosted ; mid-ocean ridge ; ecogeochemistry

58 **\body**

59

60 **Introduction**

61 High-temperature hydrothermal vents occur at very geographically restricted sites in the deep-
62 sea, localized on spreading ridges and arc-related volcanoes. Typically, such vent fluids are
63 metal- and H₂S-rich, and precipitate metallic sulfide chimneys on the seafloor(1, 2). These
64 vents usually support high-biomass invertebrate communities, dominated by a small number
65 of endemic species forming symbioses with diverse chemoautotrophic bacteria (e.g.
66 siboglinid tube worms, bresiliid shrimp, provaniid gastropods, vesicomid clams and
67 bathymodiolin mussels)(1, 3). These symbioses exploit chemical energy from a variety of
68 fluids enriched in reduced compounds, mostly hydrogen sulfide and methane, to fix
69 carbon(4). Along slow and ultraslow spreading ridges, like the Mid-Atlantic Ridge (MAR),
70 ultramafic mantle rocks can be exposed on the seafloor by large offset faults(5). Seawater
71 serpentinization of these peridotites produces hydrogen, which subsequently reacts with CO₂
72 to form methane(6, 7). Because of this, peridotite-hosted high-temperature vent sites on the
73 MAR (e.g. Rainbow and Logatchev) exhibit elevated levels of methane and hydrogen
74 contents in their fluids. Hydrothermal activity can also occur at off-axis ridge settings. A
75 unique example of this is the Lost City vent field, discovered in the year 2000 on the Atlantis
76 Massif, 30°07'N MAR, at 750-850 m(8). Here, exothermic serpentinization processes may
77 largely drive the hydrothermal convection, although a contribution of magmatic inputs is not
78 excluded(9). The main difference between this off-axis vent field and the other known vent
79 fields on the MAR-axis is that the majority of the Lost City vent fluids are metal-poor, low-
80 temperature (40-91 °C), and have high pH (9-11). Further, the Lost City fluids are also highly
81 enriched in H₂ and CH₄ and comparatively lower in H₂S(10). On contact with ambient
82 seawater these alkaline fluids precipitate chimney structures up to 60 meters-high composed

83 of carbonates (aragonite and calcite) and brucite ($Mg(OH)_2$)(11-13). Sulfide minerals are
84 mostly absent from these chimneys, contrasting strongly with on-axis hydrothermal vent
85 structures(13, 14). The Lost City site has generated considerable interest because this sort of
86 system was likely to have been common in early Earth history and represents a plausible
87 geochemical environment for the emergence of life on this, and potentially other planets(15,
88 16).

89

90 In the context of the MAR peridotite-hosted vent fields another remarkable feature of Lost
91 City is the lack of typical high-biomass animal assemblages dominated by large
92 chemosynthetic invertebrates: there are currently no *Bathymodiolus* mussel beds or bresiliid
93 shrimp swarms, although the diversity of other invertebrates (particularly small gastropods
94 and polychaete worms) is described as being equivalent to that of high-temperature MAR
95 vent communities(11, 17). Only two living specimens of *Bathymodiolus* aff. *azoricus* have
96 been found at Lost City(18, 19), whereas hundreds of broken shell fragments downslope away
97 from the active chimney areas(19, 20) suggest that the population size might have been much
98 larger in the past and is now almost extinct(19). Dead *B. azoricus* shells have also been
99 recently reported from inactive carbonate chimneys at an inactive site near Lost City (21).

100

101 Supporting these observations, the enrichment of reduced compounds in Lost City
102 hydrothermal fluid indicates that these, and similar peridotite hosted vents, hold the energetic
103 potential to support large aggregations of *Bathymodiolus* mussels, a genus widely distributed
104 along the MAR axis(22). *B. aff. azoricus* at Lost City hosts the same symbiont phylotypes as
105 the methanotrophic and thiotrophic endosymbionts of both *B. azoricus* and *B. puteoserpentis*
106 from on-axis sites on the MAR(18), where the methanotrophic symbiont fixes carbon from

107 methane and the chemolithoautotroph uses sulfide to fix CO₂(23-25). In addition to methane,
108 DeChaine et al.(18) suggest that *B. aff. azoricus* at Lost City could also be utilizing
109 hydrogen, although hydrogen-oxidizing symbionts have yet to be identified. These authors
110 further suggested that hydrogen sulfide would be poorly available for mussels at Lost
111 City(18), based on measured sulfide concentrations from Lost City end-member fluids.
112 However, this hypothesis is not supported by the comparison of the end-member total
113 dissolved sulfide versus temperature ratios between Lost City and the on-axis vent fields
114 (supporting Table S1). The maximum temperature of the habitat of *Bathymodiolus* mussels
115 lies around 15°C, and it requires significant dilution of the end-member fluids in cold
116 seawater. In this temperature range, the sulfide concentration resulting from the dilution of
117 Lost City end-member should be rather similar to the levels experienced by mussels from on-
118 axis vent fields(22, 26). Recent data(27), moreover, suggest that fluids issuing from flanges
119 on the flanks of Lost City chimneys may indeed have a higher H₂S/temperature ratio than the
120 end-member fluid. Given the potential availability of these reduced compounds in the Lost
121 City vent fluids for symbionts and free-living chemotrophic microbial populations(28, 29),
122 there is therefore no reason to suppose that Lost City type fluids should exclude the formation
123 of dense chemosynthetic faunal assemblages.

124

125 The findings contained in this paper support the hypothesis that Lost City type fluids can
126 sustain such communities, while providing further evidence for the suggestions of Kelley et
127 al.(17, 30) that low-temperature hydrothermal circulation on slow-spreading ridges has a
128 widespread distribution. We report for the first time Lost City-like carbonates containing
129 fossil *Bathymodiolus* shells of large size at high densities, together with smaller numbers of
130 two species of chemosynthetic bivalves and four gastropod species. This fossil assemblage is
131 110,000 years old (based on radiogenic isotopes) and contains similar species to the

132 *Bathymodiolus* mussel beds from high-temperature vents elsewhere on the MAR. Although
133 geographically close to the Rainbow hydrothermal vent field, the Ghost City carbonates and
134 fossils were clearly associated with a distinct type of environment associated with metal-poor
135 fluid venting, contrasting with all known MAR axis high-temperature vent fluids. This finding
136 not only reveals the existence of low-temperature hydrothermal circulation in serpentinized
137 systems driving substantial fluxes of reduced chemicals close to the ridge axis, but it also
138 expands the range of marine environments that can support chemosynthetic animal
139 communities.

140

141 **Ghost City carbonates**

142 Eight carbonate blocks were dredged during the MoMARDREAM cruise (MoMAR 08 Leg 2,
143 August-September 2008) from the north-western flank of the Rainbow massif, which is
144 situated on a non-transform offset at 36°14.15N, 33°53.50W (Figure 1 and supporting figure
145 S1). This site, which we name Ghost City, is 1200 m north-east of the Rainbow vent field at
146 around 2100 m water depth. The dredge from which the carbonates were collected sampled a
147 transect around 800 m long on the seafloor and recovered, in addition to the carbonates, three
148 shells of thyasirid bivalves, numerous pieces of serpentinized peridotite, and some troctolites
149 and gabbros. The carbonates are white to ivory in colour, ranging from 750 to 25 cm³ in
150 volume, and most have thin (up to 1 mm) exterior ferric oxyhydroxide (ferrihydrite with Mn
151 component) black crusts upon which solitary corals have grown (Figure 2A-B and supporting
152 figure S2). The carbonate textures range from 'layered' (Figure 2C and supporting figure S3),
153 with significant porosity (close to 40%, n = 4), to 'massive'. This carbonate matrix which
154 encrusts mussel shells with a density of up to 4 shells per 10 cm³, lacks metallic oxide or
155 sulfide minerals and consists of varying proportions of authigenic carbonate cements, and
156 infilling pelagic calcitic and aragonitic fossils (foraminifera, coccoliths and a few pteropods;

157 Figure 2D and supporting figures S3). The authigenic carbonate cements consist of aragonite,
158 commonly occurring as radial aggregates of acicular crystals, calcite, and sparser rosettes of
159 glendonite crystals (Figure 2E-F and supporting figure S4). The infilling pelagic sediments
160 have $\delta^{18}\text{O}$ values of $3.63 \pm 0.25\text{‰}$ and $\delta^{13}\text{C}$ values of $0.93 \pm 0.17\text{‰}$ ($n = 4$). Mixed
161 calcite/aragonite authigenic cements have $\delta^{18}\text{O}$ and $\delta^{13}\text{C}$ values of $4.88 \pm 0.19\text{‰}$ and $-0.66 \pm$
162 1.18‰ , respectively ($n = 9$) (Table 1). The authigenic carbonates and the in-filled pelagic
163 sediment show good separation between $\delta^{13}\text{C}$ and $\delta^{18}\text{O}$ on a Canonical Discriminant Analysis
164 (CDA) scatterplot, supporting distinct mineralization process (Figure 3 and supporting table
165 S2). Isotopic measurements of a series of subsamples from one authigenic carbonate crust
166 gave U/Th ages ranging from 46 ± 0.3 kyr to 193 ± 11 kyr ($n = 4$) (Table 2). These samples
167 however display a wide range of initial $\delta^{234}\text{U}$ values (from ~ 129 to 183‰), suggesting that
168 their U/Th ages may be possibly biased due to post-formation interaction with seawater or
169 diagenesis(31). One of these subsamples is characterized by a $\delta^{234}\text{U}_{\text{initial}}$ value ($150 \pm 1\text{‰}$,
170 Table 2) close to the modern seawater signature ($146.6 \pm 2.6\text{‰}$)(31), which suggests that its
171 U/Th ratio may be considered as the most representative of the formation age of Ghost City
172 carbonates. The corresponding U/Th age (110 ± 0.9 kyr) lies in the same range than the older
173 chimneys from Lost City (122 ± 12 kyr)(32), and suggests that Ghost City carbonate
174 formation is significantly older than the first evidence of Rainbow vent activity (23 ± 1.5
175 kyr)(33). Additionally, the same carbonate sample exhibits a radiogenic strontium isotopic
176 ratio ($^{87}\text{Sr}/^{86}\text{Sr}$) of 0.70916 ± 0.00006 , close to seawater ratios.

177

178 Among known authigenic carbonates from oceanic environments where ultramafic rocks are
179 exposed, such as vein-filling aragonites in serpentinites(34, 35), samples from Ghost City are
180 texturally and mineralogically most similar to those from Lost City, particularly the
181 carbonates of old (up to 25 kyr) inactive chimneys(12). According to these authors, the Lost

182 City inactive structures display well-defined fluid flow paths, retaining significant porosity
183 (up to ~35%) and are characterized by dark or black exteriors which contrast to white, ivory
184 or gray interiors. The outer walls of these structures become dark due to manganese
185 precipitation associated with aging, and are colonized by serpulid worms and corals(13). In
186 older inactive chimneys the internal microchannels are progressively in-filled with micritic
187 calcite; brucite, which is undersaturated in seawater, tends to disappear in these chimneys(12).
188 Another feature indicative of prolonged post-formation interaction with seawater is near
189 seawater Sr isotope values in carbonate minerals, as seen in both the Lost City inactive
190 chimneys(13) and Ghost City samples. One mineralogical distinction of Ghost City
191 carbonates is the presence of glendonite. Glendonite in Ghost City carbonate crust exhibits a
192 classical star-shape and is associated with acicular aragonite crystals surrounding the benthic
193 fossils. Glendonite is a pseudomorph after ikaite, a very unstable hydrous calcium carbonate
194 associated with cold water (<6°C) depositional systems, including glaciomarine and deep
195 water settings(36, 37). Original ikaite precipitation is favoured by elevated alkalinity, high pH
196 (>10) and dissolved phosphate enrichments. Glendonite was not reported in Lost City
197 carbonates, but the presence of ikaite in the walls of active chimneys was suspected from the
198 observation of rapid dissolution of elongated carbonate crystals during sampling(13).
199 The oxygen and carbon isotope values of the Ghost City authigenic carbonates are consistent
200 with those observed in serpentinization contexts. The ¹⁸O enrichment during fluid/rock
201 interaction results in carbonates with high δ¹⁸O values (>2‰)(11, 38). The Ghost City carbon
202 isotope signatures (δ¹³C = -2.6 to 0.7‰) are comparable to those measured in carbonates
203 from serpentinite-hosted ecosystems, like the South Chamorro Seamount (δ¹³C = -2.1 to -1.3
204 ‰) and the Conical Seamount (δ¹³C = -2.9 to -0.1 ‰) in the Mariana forearc(39-41), and lie
205 within the wide range of carbonate isotopic signatures reported for Lost City (-7 to
206 +13‰)(11). Carbonates with the lower isotopic signature reflect a mixed inorganic carbon

207 source with contributions from seawater ($\delta^{13}\text{C}_{\text{DIC}} \sim 0\text{‰}$) and an isotopically lighter-DIC
208 source. Owing to the very low concentration of inorganic carbon in serpentinization fluids,
209 the most likely origin for this ^{13}C depleted DIC is the oxidation of methane. Methane in
210 serpentinization fluids are characterized by light carbon isotopic signatures (e.g., $\delta^{13}\text{C}_{\text{CH}_4} =$
211 -7‰ in Zambales ophiolites seeps, -10.3‰ at Logatchev, -16.7‰ at Rainbow, -11.9‰ at
212 Lost City)(42-45), which can be further fractionated by methanotrophic microbes converting
213 methane into inorganic carbon. While abiotic methane oxidation is kinetically inhibited at low
214 temperature(46), microbial oxidation of methane can occur in subseafloor habitats with
215 various electron acceptors (e.g. oxygen and sulphate) during the mixing of seawater with end-
216 member fluids(47, 48). According to Proskurowski et al.(48), the fractionation factor resulting
217 of anaerobic or aerobic methane oxidation can be as high as 1.039(49, 50) and will results in
218 further depletion of the initial carbon isotopic ratio by at least -13‰ . Only a small fraction
219 ($\sim 5\%$) of this ^{13}C depleted methane is thus sufficient to explain the slightly negative carbon
220 isotopic signature of some Ghost City carbonates. An additional contribution from biogenic
221 methane formed during the subseafloor mixing of seawater and the end-member fluid, as
222 described in Proskurowski et al.(48) cannot be ruled out. This assumption is supported by the
223 identification of both methanogenic and anaerobic methane-oxidizing *Archea* at Lost City,
224 particularly in the less active chimneys where seawater mixing is occurring(28). In Lost City-
225 type conditions, seawater is the only source of HCO_3^- and mixing is required to compensate
226 the poor supply of this ion from the fluid. As a consequence, the substantial isotopic
227 fractionation resulting of biogenic methane formation that was observed at basalt-hosted
228 diffuse vents(48) may not be achieved due to limiting inorganic carbon conditions. The
229 relative importance of biogenic methane is therefore difficult to estimate from Ghost City
230 samples isotopic ratios.

231

232 The geological context, as well as petrographic and isotopic data, provides supporting
233 evidence that the Ghost City carbonates were formed 110,000 years ago from venting of
234 metal-poor fluids. Despite the proximity with the Rainbow high-temperature vents field, the
235 lack of polymetallic sulfide precipitates in the Ghost City carbonate samples precludes a high-
236 temperature metal-rich hydrothermal fluid contribution in their formation. More likely, these
237 fluids were formed from low temperature hydrothermal circulation related to serpentinization
238 and were probably close in composition to those currently venting at Lost City.

239

240 **Ghost City fossils**

241 We counted 146 specimens of the mussel *Bathymodiolus* aff. *azoricus* on the exposed
242 surfaces of the eight Ghost City carbonate blocks (Figure 4 and supporting information figure
243 S4). The shells range in length from 5 mm to 84 mm, which is comparable to living *B.*
244 *azoricus* shells from high-temperature hydrothermal vent fields on the MAR(51). Very few of
245 the Ghost City mussel shells are fragmented and quite a few specimens have articulated
246 valves, with a ratio of 3.6 disarticulated to articulated shells (n = 73). Some of the small
247 articulated mussel shells are nested within larger articulated specimens (Figure 2-D). These
248 features are indicative of in-situ growth and a lack of post mortem transport. This
249 interpretation is supported by the isotope composition of the Ghost City *B.* aff. *azoricus* shells
250 ($\delta^{18}\text{O} = 4.93 \pm 0.40\text{‰}$, $\delta^{13}\text{C} = -0.30 \pm 1.99\text{‰}$, n = 3; Table 1), values which are more similar
251 to the Ghost City authigenic carbonates than living *Bathymodiolus* shells from the Rainbow
252 high-temperature hydrothermal vent site (CDA analysis, Figure 3 and supporting table S2).
253 The other benthic fossils enclosed within the Ghost City carbonate samples (Figure 4)
254 comprise serpulid tubes (> 30), the vesicomid clam *Phreagena* sp.(n = 2), thyasirid clam
255 *Thyasira* sp. (n = 1), the limpet *Paralepetopsis* aff. *ferrugivora* (n = 15) and the snails
256 *Protolira* aff. *thorvaldssoni* (n = 32), *Phymorhynchus* sp. (n = 1), *Anatoma* sp. (n = 2) and

257 *Lurifax vitreus* (n = 1). These also show variable preservation, but in general the shells that
258 were originally aragonitic (the gastropods and clams) show more dissolution and
259 recrystallization than the mixed calcite/aragonite mussel shells, an observation consistent with
260 prolonged seawater interaction (Supporting figure S5). The Ghost City mollusk assemblage
261 shares five taxa with living MAR axial high-temperature vent communities(3, 52-54),
262 including two locally at Rainbow (*Bathymodiolus* and *Protolira*), and two taxa associated
263 with sedimented vent sites (supporting information table S3). The Ghost City *Phreagena* sp.
264 is also found at the recently described Clamstone site, an inactive (~25 kry BP) serpentine-
265 hosted sedimented vent field near Rainbow (approximately 1.2 km east of Ghost City, at a
266 depth of 1980 m)(55). Thyasirid clams that may be conspecific with the Ghost City *Thyasira*
267 sp. occur at Clamstone(55), Anya's Garden, a sedimented vent site in the Logatchev area(52,
268 56, 57), and have also been reported in soft sediments at Lost City(20). Thus, the Ghost City
269 mollusk fauna is a mixture of MAR vent species from sedimented sites and more typical
270 chimney habitat mussel bed communities. Although Ghost City fauna has a higher biomass,
271 the mollusc species list is not greatly different from Lost City communities, with three
272 mollusk species shared between the two sites: *B. azoricus*, *Thyasira* species and the gastropod
273 *Lurifax*; see supporting information table S3).

274

275 **High-biomass vent communities supported by serpentinization fluids**

276 The Ghost City carbonates demonstrate that 1) high-biomass populations of *Bathymodiolus*
277 mussels, and other symbiont-hosting mollusks can be supported by metal-depleted and likely
278 alkaline fluids, similar to the serpentinization-related vent fluids described at Lost City, and 2)
279 these communities have been present on the axis of the MAR for at least 110,000 years. The
280 flexible *B. azoricus* dual symbiosis responds to variations in the methane to sulfide ratio in the
281 environment(24, 25) making this species particularly well adapted to the variety of fluid

282 chemistries that are found on the MAR(8, 58). The Ghost City fossil mussels might therefore
283 also have relied on methanotrophy and, potentially, on sulfide, or even hydrogen, oxidation as
284 primary energy pathways. Although the geological setting is different, there is evidence that
285 some other *Bathymodiolus* species are able to exploit diverse energy sources present in a
286 serpentinization context. At the South Chamorro serpentinite seamount in the Mariana forearc
287 mussels thrive in sedimented cracks in seafloor carbonate cement, and based on soft tissue
288 carbon and sulfur isotopic data, Yamanaka et al.(41) suggest that the mussels host both
289 methanotrophic and thiotrophic symbionts, utilizing both methane from serpentinization
290 reactions and sulfur produced by sulfate reducing bacteria in the sediment. Additionally,
291 vesicomysids(4, 59) and many of the studied large thyasirid(4, 52) species host sulfide-
292 oxidizing symbionts, and the presence of representative species in the Ghost City carbonates
293 suggests that a threshold amount of sulfide was present in the Ghost City environment.

294

295 **Implications**

296 It is unclear why communities of symbiont-hosting molluscs, including high densities of large
297 *Bathymodiolus* mussels, do not currently persist at Lost City, when they have been present in
298 the past as shown by accumulations of dead shells. Because *Bathymodiolus azoricus* is able to
299 exploit variable chemical energy sources, the most likely explanation is to be searched for in
300 the ecological processes that govern community dynamics in fragmented habitats. One
301 possible cause of this extinction may be related to the dispersal potential of vent species. Lost
302 City is located further from the ridge axis than Ghost City and may have lacked of sufficient
303 larval flow from high-temperature Rainbow-like vent field communities after a major
304 disturbance event. Another explanation could be that the focused flow chimney complex at
305 Lost City lacks the mild temperature diffuse flow areas (< 15°C) with substantial
306 concentrations of electron donors like methane or sulfide, that characterize suitable habitat for

307 vent mussels(22). Further investigation of Lost City habitat conditions and population
308 genetics will help discriminating between these hypotheses.
309 The findings further support the hypothesis of a widespread occurrence of hydrothermal fluid
310 circulation hosted in exposed ultramafic rocks on the ocean floor(60). The estimated duration
311 of serpentinization-related fluid venting (over 10 kyr to 100 kyr timescales)(32) contrast
312 strongly with the geographically restricted and short-lived high-temperature vent fields known
313 to date. Our results indicate that exposed mantle rocks undergoing serpentinization could host
314 deep-sea chemosynthetic vent communities in a wide range of geological settings, including
315 slow and ultraslow spreading ridge axes, off-axis Oceanic Core Complexes(61), continental
316 margins(62) and serpentinite seamounts in forearc settings(63). The exploration of ultramafic
317 rock exposures in the deep-sea is thus a fertile area for the understanding both long-range
318 larval dispersal of vent species, and the specific requirements for settlement and growth of
319 chemosynthetic animals.

320

321 **Methods**

322 **XRD analyses**

323 Analyses of carbonate matrix, oxide crust and mussel shells were made at the ISTeP
324 laboratory (UPMC Univ Paris 06) on a Siemens D501. *Bathymodiolus* aff. *azoricus* mussel
325 shells were scrubbed in distilled water with a toothbrush immediately upon collection to
326 remove loosely attached biogenic and inorganic particles. Sample powders of original calcitic
327 outer layer and aragonitic inner layer of the shells were drilled from a depth of ~0.1 mm.

328 **Optical petrography**

329 Polished thin sections of carbonates were observed using a stereomicroscope Zeiss SteREO
330 Discovery V20 (Figs. 2 and S1) Porosity measurements were made using JMicrovision
331 software (www.jmicrovision.com).

332 **Carbon and oxygen stable isotopes analyses**

333 Analyses of three *Bathymodiolus* aff. *azoricus* shells and thirteen carbonate matrix (authigenic
334 carbonate and infilling pelagic sediments) Ghost City samples were made on a VG
335 Micromass 602 mass spectrometer. Additionally, five shells of living *B. azoricus* from the
336 Rainbow vent field were analyzed. Powdered samples from mussel shells for the isotopic
337 analyses (3-4 mg) were obtained from the cleaned outer layer using a rotary drill with a
338 diamond-tipped burr. The shell sample powders were pre-treated with 1.5 % NaClO for 30
339 min to remove organic contaminants, rinsed three times with distilled water following a
340 protocol modified after(64, 65). All carbonate powders were acidified in 100% phosphoric
341 acid at 50°C under vacuum. The produced CO₂ was collected and analysed using the mass
342 spectrometer. Isotopic data are reported in conventional delta (δ) notation relative to the
343 Vienna Pee Dee Belemnite (VPDB). The standard used for the analyses was an internal
344 standard calibrated on the NBS-19. Standard deviation for δ¹⁸O and δ¹³C is ± 0.10‰.

345 **Uranium/Thorium and strontium analyses**

346 Analyses were made in the Pôle Spectrométrie Océan (Brest) on a Neptune MC-ICPMS. For
347 uranium and thorium isotope measurements, about 2 mg of carbonate sample were dissolved
348 in 7.5M HNO₃ and spiked with a mixed ²³⁶U/²²⁹Th spike(66). U and Th were separated
349 chemically using conventional anion exchange techniques adapted from previous studies(67).
350 U and Th concentrations and isotope ratios were then measured in the MC-ICPMS. The
351 carbonate age was corrected for detrital contamination (inherited ²³⁰Th) using measured ²³²Th
352 concentrations and assuming a typical ²³²Th/²³⁰Th ratio (150,000) for the contaminant detrital
353 phase, but this correction was insignificant on the calculated age (about 1 %)(68). Strontium
354 was isolated using Sr resin and the isotope ratios were measured using the MC-ICPMS.
355 Isotope ratios were normalised to ⁸⁶Sr/⁸⁸Sr=0.1194 and corrected from ⁸⁷Rb and ⁸⁶Kr
356 interferences on the ⁸⁷Sr and ⁸⁶Sr signal, respectively.

357

358 **Acknowledgments**

359 We thank Captain and crew of R/V L'Atalante, the ROV Victor operation group, and the
360 MoMARDREAM scientific party for their support during the MoMARDREAM cruise.
361 CNRS-INSU, CNRS-INEE, IFREMER and GENAVIR are gratefully acknowledged for their
362 financial and technical support. The study was part of the CHEMECO collaborative project
363 from the ESF EUROCORES EURODEEP and benefited from the joint support of Fondation
364 TOTAL and UPMC to the chair 'Extreme environment, biodiversity and global change'. The
365 authors thank E. Rongemaille, N.-C. Chu and E. Ponzevera for analytical work, E. Krylova
366 for vesicomid and thyasirid bivalve identification, and A. Wären for benthic gastropod
367 identification. T.M. Shank and A.L. Meistertzheim are also thanked for their helpful
368 comments and. The manuscript also benefited from helpful comments from G. Proskurowski
369 and one anonymous reviewer.

370

371 **References**

- 372 1. Van Dover CL (2000) *The ecology of deep-sea hydrothermal vents* (Princeton
373 University Press, Princeton).
- 374 2. Von Damm KL (1990) Seafloor hydrothermal activity: black smoker chemistry and
375 chimneys. *Annual Review of Earth and Planetary Sciences* 18:173-204.
- 376 3. Desbruyères D, Segonzac M, Bright M (2006) *Handbook of deep-sea hydrothermal*
377 *vent fauna - Mollusca* (Denisia, Linz) pp 141-172.
- 378 4. Dubilier N, Bergin C, Lott C (2008) Symbiotic diversity in marine animals: the art of
379 harnessing chemosynthesis. *Nat. Rev. Microbiol.* 6:725-740.
- 380 5. Cannat M (1993) Emplacement of mantle rocks in the seafloor at mid-ocean ridges *J.*
381 *Geophys. Res.* 98:4163-4172.

- 382 6. Abrajano TA, et al. (1988) Methane-hydrogen gas seeps, Zambales Ophiolite,
383 Philippines: deep or shallow origin? *Chem. Geol.* 71:211-222.
- 384 7. Berndt ME, Allen DE, W.E. S (1996) Reduction of CO₂ during serpentinization of
385 olivine at 300°C and 500 bar. *Geology* 24:351-354.
- 386 8. Kelley DS, et al. (2001) An off-axis hydrothermal vent field near the Mid-Atlantic
387 Ridge at 30°N. *Nature* 412:145-149.
- 388 9. Allen DE, Seyfried Jr. WE (2004) Serpentinization and heat generation: constraints
389 from Lost City and Rainbow hydrothermal systems. *Geochim. Cosmochim. Acta*
390 68:1347-1354.
- 391 10. Proskurowski G, Lilley MD, Kelley DS, Olson EJ (2006) Low temperature volatile
392 production at the Lost City Hydrothermal Field, evidence from a hydrogen stable
393 isotope geothermometer. *Chem. Geol.* 229:331-343.
- 394 11. Kelley DS, et al. (2005) A serpentinite-hosted ecosystem: the Lost City hydrothermal
395 field. *Science* 307:1428-1434.
- 396 12. Früh-Green GL, et al. (2003) 30,000 years of hydrothermal activity at the Lost City
397 vent field. *Science* 301:495-498.
- 398 13. Ludwig KA, Kelley DS, Butterfield DA, Nelson BK, Früh-Green GL (2006)
399 Formation and evolution of carbonate chimneys at the Lost City Hydrothermal Field.
400 *Geochim. Cosmochim. Acta* 70:3625-3645.
- 401 14. Fouquet Y, et al. (1993) Tectonic setting and mineralogical and geochemical zonation
402 in the Snake Pit sulfide deposit (Mid-Atlantic Ridge at 23°N). *Econ. Geol.* 88:2018-
403 2036.
- 404 15. Holm NG, Charlou JL (2001) Initial indications of abiotic formation of hydrocarbons
405 in the Rainbow ultramafic hydrothermal system, Mid-Atlantic Ridge. *Earth Planet.*
406 *Sci. Lett.* 191:1-8.

- 407 16. Sleep NH, Meibom A, Fridriksson T, Coleman RG, Bird DK (2004) H₂-rich fluids
408 from serpentinization: geochemical and biotic implications. *PNAS* 101:12818-12823.
- 409 17. Kelley DS, Früh-Green GL, Karson JA, Ludwig KA (2007) The Lost City
410 hydrothermal field revisited. *Oceanography* 20:90-99.
- 411 18. DeChaine EG, Bates AE, Shank TM, Cavanaugh CM (2006) Off-axis symbiosis
412 found: characterization and biogeography of bacterial symbionts of *Bathymodiolus*
413 mussels from Lost City hydrothermal vents. *Environ. Microbiol.* 8:1902-1912.
- 414 19. Shank TM, Buckman KL, Butterfield D, Kelley D (2006) Macrofaunal
415 characterization of peridotite-hosted ecosystems associated with Lost City
416 hydrothermal field. *Eos. Trans. AGU, Ocean Sci. Meet. Suppl.* 87:OS10-35.
- 417 20. Gebruk AV, Galkin SV, Krylova EM, Vereshchaka AL, Vinogradov VM (2002)
418 Hydrothermal fauna discovered at Lost City (30°N, Mid-Atlantic Ridge). *InterRidge*
419 *News* 11:18-19.
- 420 21. Dara OM, Kuz'mina TG, Lein AY (2009) Mineral associations of the Lost Village and
421 Lost City hydrothermal fields in the North Atlantic. *Oceanology* 49:688-696.
- 422 22. Le Bris N, Duperron S (2010) Chemosynthetic communities and biogeochemical
423 energy pathways along the MAR: the case of *Bathymodiolus azoricus*. *Diversity of*
424 *hydrothermal systems on slow-spreading ocean ridges*, eds Rona PA, Devey CW,
425 Dymont J, & Murton BJ (AGU Geophysical Monograph Series, Washington), Vol
426 188, pp 409-429.
- 427 23. Fiala-Medioni A, et al. (2002) Ultrastructural, biochemical, and immunological
428 characterization of two populations of the mytilid mussels *Bathymodiolus azoricus*
429 from the Mid-Atlantic Ridge: evidence for a dual symbiosis. *Mar. Biol.* 141:1035-
430 1043.

- 431 24. Duperron S, et al. (2006) A dual symbiosis shared by two mussel species,
432 *Bathymodiolus azoricus* and *Bathymodiolus puteoserpentis* (Bivalvia: Mytilidae),
433 from hydrothermal vents along the northern Mid-Atlantic Ridge. *Environ. Microbiol.*
434 8:1441-1447.
- 435 25. Riou V, et al. (2008) Influence of chemosynthetic substrates availability on symbiont
436 densities, carbon assimilation and transfer in the dual symbiotic vent mussel
437 *Bathymodiolus azoricus*. *Biogeosci. Disc.* 5:2279-2304.
- 438 26. Desbruyères D, et al. (2001) Variations in deep-sea hydrothermal vent communities
439 on the Mid-Atlantic Ridge near the Azores plateau. *Deep Sea Res. I* 48:1325-1346.
- 440 27. Konn C, et al. (2009) Hydrocarbons and oxidized organic compounds in hydrothermal
441 fluids from Rainbow and Lost City ultramafic-hosted vents. *Chem. Geol.* 258:299-
442 314.
- 443 28. Brazelton WJ, Schrenk MO, Kelley DS, Baross JA (2006) Methane- and sulfur-
444 metabolizing microbial communities dominate the Lost City hydrothermal field
445 ecosystem. *Appl. Environ. Microbiol.* 72:6257-6270.
- 446 29. Brazelton WJ, et al. (2010) Archaea and bacteria with surprising microdiversity show
447 shifts in dominance over 1,000-year time scales in hydrothermal chimneys. *PNAS*.
- 448 30. Cannat M, Fontaine F, Escartin J (2010) Serpentinization and associated hydrogen and
449 methane fluxes at slow spreading ridges. *Diversity of hydrothermal systems on slow*
450 *spreading ocean ridges*, eds Rona PA, Devey CW, Dymont J, & Murton BJ (AGU
451 Geophysical Monograph Series, Washington), Vol 188, pp 241-264.
- 452 31. Robinson LF, Belshaw NS, Henderson GM (2004) U and Th concentrations and
453 isotope ratios in modern carbonates and waters from the Bahamas. *Geochim.*
454 *Cosmochim. Acta* 68:1777-1789.

- 455 32. Ludwig KA, Shen C, Kelley DS, Cheng H, Edwards RL (2009) U-Th isotopic
456 systematics and ages of carbonate chimneys at the Lost City hydrothermal field. *Eos.*
457 *Trans. AGU, Fall Meet. Suppl.* 90:V31D-2007.
- 458 33. Kuznetsov K, et al. (2006) $^{230}\text{Th}/\text{U}$ dating of massive sulfides from the Logatchev and
459 Rainbow hydrothermal fields (Mid-Atlantic Ridge). *Geochronometria* 25:51-55.
- 460 34. Eickmann B, Bach W, Peckmann J (2009) Authigenesis of carbonate minerals in
461 modern and Devonian ocean-floor hard rock. *The Journal of Geology* 117:307-323.
- 462 35. Ribeiro Da Costa I, Barriga FJAS, Taylor RN (2008) Late seafloor carbonate
463 precipitation in serpentinites from the Rainbow and Saldanha sites (Mid-Atlantic
464 Ridge). *Eur. J. Mineral.* 20:173-181.
- 465 36. Buchardt B, et al. (1997) Submarine columns of ikaite tufa. *Nature* 390:129-130.
- 466 37. Selleck BW, Carr PF, Jones BG (2007) A review and synthesis of glendonites
467 (pseudomorphs after ikaite) with new data: assessing applicability as recorders of
468 ancient coldwater conditions. *Journal of Sedimentary Research* 77:980-991.
- 469 38. Mével C (2003) Serpentinization of abyssal peridotites at mid-ocean ridges. *C.R.*
470 *Geoscience* 335:825-852.
- 471 39. Haggerty JA (1991) Evidence from fluid seeps atop serpentine seamounts in the
472 Mariana forearc: clues for emplacement of the seamounts and their relationship to
473 forearc tectonics. *Mar. Geol.* 102:293-309.
- 474 40. Kato K, Wada H, Fujioka K (1998) Carbon and oxygen isotope composition of
475 carbonate chimney from Mariana forearc seamount. *JAMSTEC J. Deep Res.* 14:213-
476 222.
- 477 41. Yamanaka T, et al. (2003) Stable isotope evidence for a putative endosymbiont-based
478 lithotrophic *Bathymodiolus* sp. mussel community atop a serpentine seamount.
479 *Geomicrobiol. J.* 20:185-197.

- 480 42. Abrajano TA, et al. (1990) Geochemistry of reduced gas related to serpentinization of
481 the Zambas ophiolite, Philippines. *Appl. Geochem.* 5:625-630.
- 482 43. Lilley MD, et al. (1993) Anomalous CH₄ and NH₄⁺ concentrations at unsedimented
483 mid-ocean-ridge hydrothermal system. *Nature* 364:45-47.
- 484 44. Charlou JL, et al. (2010) High production and fluxes of H₂ and CH₄ and evidence of
485 abiotic hydrocarbon synthesis by serpentinization in ultramafic-hosted hydrothermal
486 systems on the Mid-Atlantic Ridge. *Diversity of hydrothermal systems on slow-
487 spreading ocean ridges*, eds Rona PA, Devey CW, Dymont J, & Murton BJ (AGU
488 Monograph Series, Washington), pp 265-296.
- 489 45. Proskurowski G, et al. (2008) Abiogenic hydrocarbon production at Lost City
490 hydrothermal field. *Science* 319:604-607.
- 491 46. Webley PA, Tester JW (1991) Fundamental kinetics of methane oxidation in
492 supercritical water. *Energy and Fuels* 5:411-419.
- 493 47. Valentine DL, Reeburgh WS (2000) New perspectives on anaerobic methane
494 oxidation. *Environ. Microbiol.* 2:477-484.
- 495 48. Proskurowski G, Lilley MD, Olson EJ (2008) Stable isotopic evidence in support of
496 active microbial methane cycling in low-temperature diffuse flows vents at 9°50'N
497 East Pacific Rise. *Geochim. Cosmochim. Acta* 72:2005-2023.
- 498 49. Whiticar MJ, Faber E (1986) Methane oxidation in sediment and water column
499 environments - Isotopic evidence. *Org. Geochem.* 10:759-768.
- 500 50. Templeton AS, Chu KH, Alvarez-Cohen L, Conrad ME (2006) Variable carbon
501 isotope fractionation expressed by aerobic CH₄-oxidizing bacteria. *Geochim.
502 Cosmochim. Acta* 70:1739-1752.

- 503 51. Comtet T, Desbruyères D (1998) Population structure and recruitment in mytilid
504 bivalves from the Lucky Strike and Menez Gwen hydrothermal vent fields (37°17'N
505 and 37°50'N on the Mid-Atlantic Ridge) *Mar. Ecol. Prog. Ser.* 163:165-177.
- 506 52. Southward EC, Gebruk AV, Kennedy H, Southward AJ, Chevaldonné P (2001)
507 Different energy sources for three symbiont-dependent bivalve molluscs at the
508 Logatchev hydrothermal site (Mid-Atlantic Ridge). *J. Mar. Biol. Ass. UK* 81:655-661.
- 509 53. Warén A, Bouchet P (2001) Gastropoda and Monoplacophora from hydrothermal
510 vents and seeps; new taxa and records. *The Veliger* 44:116-231.
- 511 54. Taylor JD, Williams ST, Glover EA (2007) Evolutionary relationships of the bivalve
512 family Thyasiridae (Mollusca: Bivalvia), monophyly and superfamily status. *J. Mar.*
513 *Biol. Assoc. U.K.* 87:565-574.
- 514 55. Lartaud F, et al. (2010) Fossil clams from a serpentinite-hosted sedimented vent field
515 near the active smoker complex Rainbow (MAR, 26°13'N): insight into the
516 biogeography of vent fauna. *Geochem. Geophys. Geosyst.* 11:Q0AE01.
- 517 56. Gebruk AV, Chevaldonné P, Shank T, Lutz RA, Vrijenhoek RC (2000) Deep-sea
518 hydrothermal vent communities of the Logatchev area (14°45'N, Mid-Atlantic Ridge):
519 diverse biotopes and high biomass. *J. Mar. Biol. Ass. UK* 80(a):383-393.
- 520 57. Oliver PG, Holmes AM (2006) New species of Thyasiridae (Bivalvia) from
521 chemosynthetic communities in the Atlantic Ocean. *J. Conchol.* 39:175.
- 522 58. Charlou JL, Donval JP, Fouquet Y, Jean-Baptiste P, Holm N (2002) Geochemistry of
523 high H₂ and CH₄ vent fluids issuing from ultramafic rocks at the Rainbow
524 hydrothermal field (36°14'N, MAR). *Chem. Geol.* 191:345-359.
- 525 59. Childress JJ, Fisher CR, Favuzzi JA, Sanders NK (1991) Sulfide and carbon-dioxide
526 uptake by the hydrothermal vent clam, *Calymene magnifica*, and its
527 chemoautotrophic symbionts. *Physiol. Zool.* 64:1444-1470.

- 528 60. Früh-Green GL, Connolly JA, Plas A (2004) Serpentinization of oceanic peridotites:
529 implications for geochemical cycles and biological activity. *The subsurface biosphere*
530 *at Mid-Ocean Ridges*, eds Wilcock WSD, DeLong EF, Kelley DS, Baross JA, & Cary
531 SC (AGU Monograph), Vol 144.
- 532 61. Ildefonse B, et al. (2007) Oceanic core complexes and crustal accretion at slow-
533 spreading ridges. *Geology* 35:623-626.
- 534 62. Hopkinson L, Beard JS, Boulter CA (2004) The hydrothermal plumbing of a
535 serpentinite-hosted detachment: evidence from the West Iberia non-volcanic rifted
536 continental margin. *Mar. Geol.* 204:301-315.
- 537 63. Alt JC, Shanks WC (2006) Stable isotope compositions of serpentinite seamounts in
538 the Mariana forearc: serpentization processes, fluid sources and sulfur
539 metasomatism. *Earth Planet. Sci. Lett.* 242:272-285.
- 540 64. Sponheimer M, Lee-Thorp JM (1999) Isotopic evidence for the diet of an early
541 Hominid, *Australopithecus africanus*. *Science* 283:368-370.
- 542 65. Ségalen L, Lee-Thorp JM (2009) Palaeoecology of late Early Miocene fauna in the
543 Namib based on $^{13}\text{C}/^{12}\text{C}$ and $^{18}\text{O}/^{16}\text{O}$ ratios of tooth enamel and ratite eggshell
544 carbonate. *Palaeogeogr., Palaeoclimatol., Palaeoecol.* 277:191-198.
- 545 66. Robinson LF, Henderson GM, Slowey NC (2002) U-Th dating of marine isotope stage
546 7 in Bahamas slope sediments. *Earth Planet. Sci. Lett.* 196:175-187.
- 547 67. Edwards RL, Chen JH, Wasserburg GR (1986) ^{238}U - ^{234}U - ^{230}Th - ^{232}Th systematics
548 and the precise measurement of time over the past 500,000 years. *Earth Planet. Sci.*
549 *Lett.* 81:175-192.
- 550 68. Bayon G, Henderson GM, Bohn M (2009) U-Th stratigraphy of a cold seep carbonate
551 crust. *Chem. Geol.* 260:47-56.

552

553

554 List of figures

555

556 Figure 1. Location of the Ghost City fossil hydrothermal field at different scales. (A) Large
557 scale map showing hydrothermal vents hosted by volcanic rocks (red dots) and gabbros and
558 peridotites (green dots); Ghost City is in the vicinity of the Rainbow hydrothermal field. (B)
559 Standard multibeam bathymetrical map of three MAR segments between 36°00 and 36°20N.
560 These segments show a typical slow-spreading axial valley offset by two non-transform
561 discontinuities. Both Rainbow and Ghost City are located at the northern end of the segment
562 centred on 36°10N. (C) High resolution multibeam bathymetric map acquired at low ship
563 speed during cruise Flores of R/V L'Atalante showing the Rainbow vent field on the western
564 flank of the Rainbow massif; the Ghost City fossil site is located on the northwestern flank of
565 this gabbroic and peridotitic structure ~1200 m north-east of the Rainbow vent field, at a
566 depth of 2100 m.

567

568 Figure 2. Carbonate samples from Ghost City. (A) Sectioned block formed of authigenic
569 carbonate cements covered by ferric oxyhydroxide dark crust upon which (B) solitary corals
570 have grown (scale bar = 1 cm). (C) Photomicrograph showing anastomosing aragonite
571 laminae defining fluid flow channels (centre and right) and a piece of mussel shell (bottom
572 left). The channels have thin aragonite walls, some with thin collomorphic coatings, other are
573 infilled with micritic carbonate. A thin rim of aragonite acicular crystals seems to be the latest
574 cement phase, covering mussel shells, channel walls (top left) and micritic infill (centre right)
575 (scale bar = 1 mm). (D) Photomicrograph showing articulated mussel specimens and
576 gastropods enclosed within authigenic carbonate (scale bar = 1 mm). (E) and (F) SEM
577 photomicrographs of carbonates showing aragonite acicular crystals (E) and rosette of
578 glendonite crystals (F) (scale bars = 20 μ m).

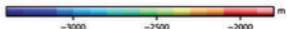
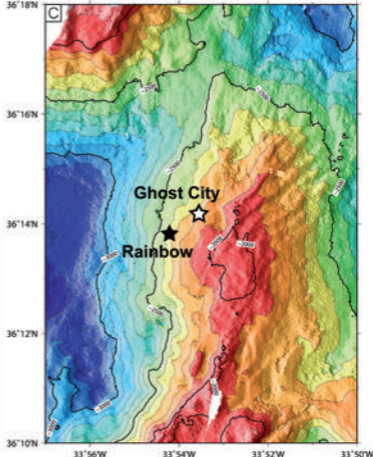
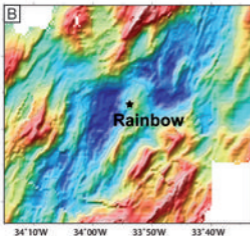
579

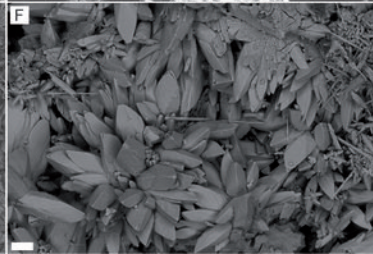
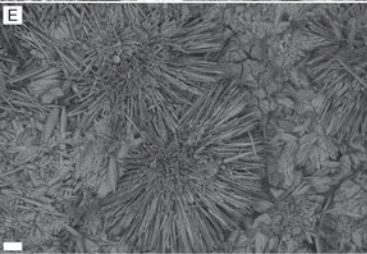
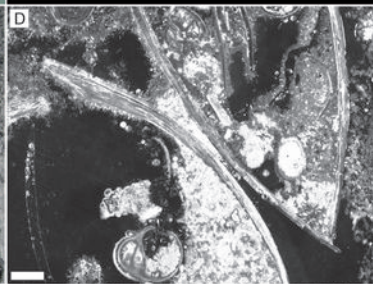
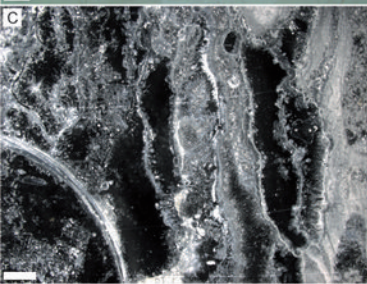
580 Figure 3. Oxygen and carbon isotopic composition of Ghost City carbonates and
581 *Bathymodiolus* shells, and living *Bathymodiolus* shells from the Rainbow hydrothermal vent
582 field. Domains limited by lines represent the scatterplot of canonical scores obtained by
583 applying discriminant functions to the data.

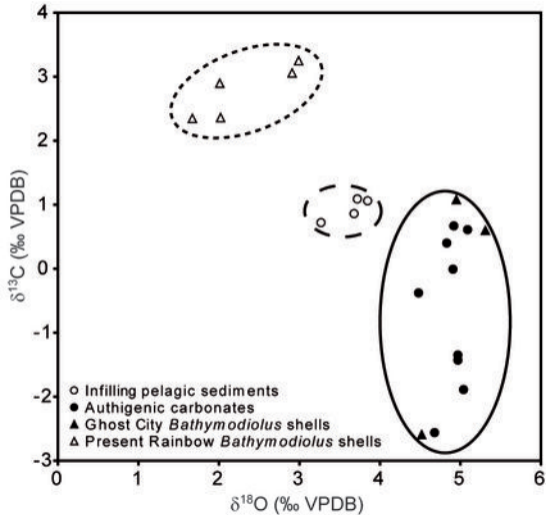
584

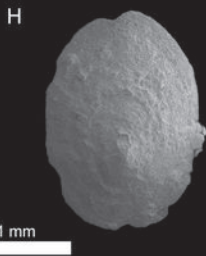
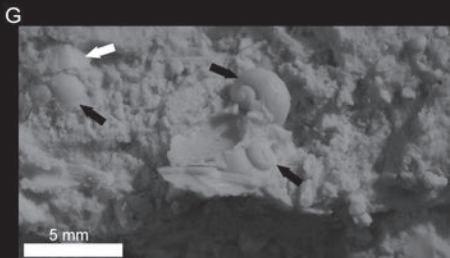
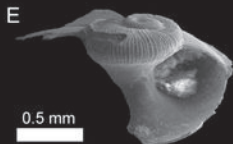
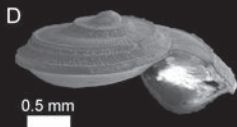
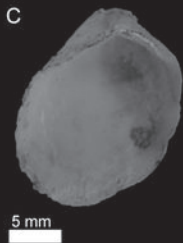
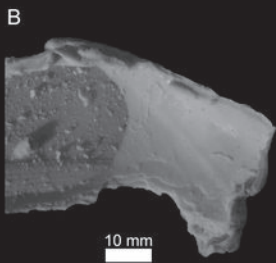
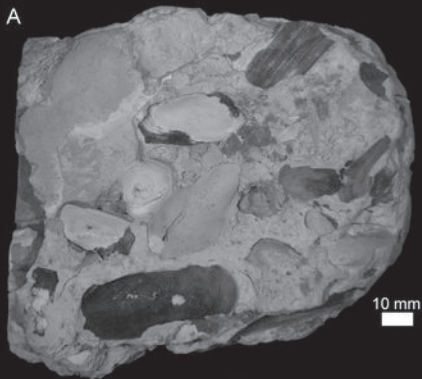
585 Figure 4. Fossils from Ghost City carbonates. (A) Carbonate block with numerous specimens
586 of *Bathymodiolus* aff. *azoricus*, showing varying degrees of shell preservation. (B) Silicone
587 rubber cast of vesicomid bivalve, right valve interior. (C) Thyasirid bivalve, left valve
588 interior. (D) Gastropod *Lurifax vitreus*, oblique apertural view. (E) Gastropod *Anatoma* sp.,
589 oblique view of damaged specimen (F) Silicone rubber cast of gastropod *Phymorhynchus* sp.,
590 side view. (G) Silicone rubber cast from carbonate containing three *Protolira* aff.
591 *thorvaldssoni* gastropod specimens (black arrows) and a single limpet (white arrow). (H)
592 Limpet *Paralepetopsis* aff. *ferrugivora*, abapertural view of slightly corroded specimen.

593









594 List of tables

595

596 Table 1: Mean, standard deviation and range of oxygen and carbon isotopic compositions of

597 carbonates and mussel shells collected in the Ghost City area, compared to Lost City

598 carbonates and living mussel shells from the Rainbow high-temperature hydrothermal vent

599 site.

600

601 Table 2: U-Th ages for Ghost City carbonate samples.

602

Table 1

	(n)	$\delta^{18}\text{O} \pm \text{SD}$		$\delta^{13}\text{C} \pm \text{SD}$	
		(‰ VPDB)	Min / Max	(‰ VPDB)	Min / Max
GHOST CITY					
Infilled pelagic sediments	4	3.63 ± 0.25	3.27 / 3.85	0.93 ± 0.17	0.72 / 1.09
Authigenic carbonates	9	4.88 ± 0.19	4.48 / 5.09	-0.66 ± 1.18	-2.56 / 0.67
<i>Bathymodiolus</i> shells	3	4.93 ± 0.40	4.52 / 5.31	-0.30 ± 1.99	-2.59 / 1.08
LOST CITY					
Vent carbonates(11)	50		-6 / 5		-7 / 13
Methane(11, 44, 45)				-11.9	-13.6 / -8.8
RAINBOW					
Living <i>Bathymodiolus</i> shells	5	2.32 ± 0.59	1.67 / 2.99	2.78 ± 0.41	2.35 / 3.25
Methane(44)					-17.7 / -15.8

Table 2

Sample	Corrected U-Th age (kyr)	Initial $\delta^{234}\text{U}$ (‰)
	$\pm 2\sigma$	$\pm 2\sigma$
S1	195 \pm 11	183 \pm 10
S2	110 \pm 0.9	150 \pm 1
S3	65 \pm 11	170 \pm 1
S4	46 \pm 0.3	129 \pm 1